Enhancing the Superconducting Transition Temperature of $BaSi_2$ by Structural Tuning

José A. Flores-Livas,[1] Régis Debord,[1] Silvana Botti,[2,1] Alfonso San Miguel,[1]
Miguel A. L. Marques,[1] and Stéphane Pailhès[1,3]

[1]*LPMCN, Université Claude Bernard Lyon I and CNRS, 69622 Villeurbanne, France*
[2]*Laboratoire des Solides Irradiés and ETSF, École Polytechnique, CNRS, CEA-DSM, 91128 Palaiseau, France*
[3]*IRM de Saclay, Laboratoire Léon Brillouin, CEA-CNRS UMR 12, CE-Saclay, F-91191 Gif-sur-Yvette, France*

(Received 4 November 2010; published 22 February 2011)

We present a joint experimental and theoretical study of the superconducting phase of the layered binary silicide $BaSi_2$. Compared with the AlB_2 structure of graphite or diboridelike superconductors, in the hexagonal structure of binary silicides the sp^3 arrangement of silicon atoms leads to corrugated sheets. Through a high-pressure synthesis procedure we are able to modify the buckling of these sheets, enhancing the superconducting transition temperature from 6 to 8.9 K when the silicon planes flatten out. By performing *ab initio* calculations based on density-functional theory we explain how the electronic and phonon properties are strongly affected by changes in the buckling. This mechanism is likely present in other intercalated layered superconductors, opening the way to the tuning of superconductivity through the control of internal structural parameters.

DOI: 10.1103/PhysRevLett.106.087002 PACS numbers: 74.70.Ad, 71.15.Mb, 74.20.−z, 74.25.Kc

Nowadays, an important part of the active research on superconductivity is focused on intercalated layered crystals. In these systems, where the relevant features for superconductivity are intrinsic to the layers, the bond buckling of the atoms forming the layers is a structural parameter known to damage the superconducting properties, regardless of the nature of the pairing mechanism [1]. The case of flat B sheets in MgB_2 is well understood: superconductivity arises from a strong coupling between the sp^2 σ-bonding intralayer electrons of B and the in-plane bond stretching phonons [2–4]. Besides, the buckling of the B honeycomb structure, as observed in ReB_2 [5], was proved to decrease the superconducting transition temperature T_c. Nevertheless, recent studies on intercalated graphite superconductors, namely (Yb, Ca)C_6 [6], and the ternary silicide CaAlSi [7,8], with high T_cs, point to the importance in these systems of the electron-phonon (EP) coupling between the interlayer electrons and the out-of-plane vibrational modes of the atoms composing the layer. In that case, the buckling phonon modes, corresponding to the antiphase motion along the c axis of the atoms in the sheets, can lead to an enhancement of the EP coupling. Experimentally, the effect of buckling can either be explored by means of high pressure or directly by chemistry. An excellent test bed for such studies is the trigonal phase of binary silicides, such as $CaSi_2$ or $BaSi_2$, which constitute a family of layered intercalated superconductors closely related to the graphite-diboride intercalated systems. Unlike the so-called AlB_2 structure of graphite-diboride compounds, where the planes are flat, in the hexagonal structure of binary silicides the Si planes buckle.

In this Letter we investigate superconductivity in $BaSi_2$ and, in particular, we focus on its layered structure ($EuGe_2$-type structure, P-3m1 space group) [9,10]. As it is sketched in the inset of Fig. 1, trigonal $BaSi_2$ is made of planes of Ba arranged in a triangular lattice, interspersed with buckled hexagonal planes of Si. This phase is metallic and was found to be superconducting with a critical temperature of 6.8 K [11]. There is every reason to expect that $BaSi_2$ is a standard s-wave superconductor, where the mechanism of superconductivity can be obtained by studying the EP coupling. However, recent theoretical studies [12] of trigonal $BaSi_2$ yielded a value of T_c almost an order of magnitude smaller than the early experimental finding of 6.8 K. These studies were based on state-of-the-art linear-response calculations within density-functional theory (DFT), that have proved to describe very accurately the superconducting properties of many other similar materials [13]. Analogous calculations for $CaSi_2$ in its trigonal high-pressure phase gave also a significant underestimation of T_c [14]. Interestingly, the application of pressure on trigonal $CaSi_2$ was shown to increase the superconducting temperature up to 14 K [15]. This finding was discussed in terms of a structural phase transition under pressure, which is expected to soften the phonon modes associated with the collapse of the corrugated Si planes [16].

In order to elucidate the origin of superconductivity in binary silicides, and at the same time to shed light on the discrepant results found in literature, we performed a joint experimental and *ab initio* study of the superconducting phase of $BaSi_2$. Our experimental data show that T_c varies strongly with the degree of buckling of the Si planes. As in the case of $CaSi_2$ [15,16], by flattening the Si planes, we increase the superconducting transition temperature T_c from 6 K up to 8.9 K. Our extensive DFT calculations allow us to determine how the buckling of the Si planes impacts the electronic and phonon band structures, and

finally the EP coupling. Through the comparison of experimental and theoretical results we infer that a soft phonon mode corresponding to the out-of-plane Si vibrations, and very sensitive to buckling, is responsible for the relatively high value of T_c in $BaSi_2$ when Si planes get flatter. Moreover, our calculations put in evidence a correlation between the softening of this phonon mode and the Si-Si bond buckling. We expect that such a behavior is a general property of conventional superconductors presenting corrugated layers.

Polycrystalline metastable high-pressure and high-temperature trigonal samples of $BaSi_2$ were synthesized in a Belt-type apparatus from the commercial (Cerac incorporated) orthorhombic phase of $BaSi_2$ (*Pnma* space group) with a purity of 98%. Different trigonal structures were metastabilized by changing the temperature and the pressure conditions of synthesis according to the phase diagram of $BaSi_2$ [9,17,18]. The structural characterizations were performed by x-ray diffraction θ-2θ measurements done on a Bruker D8 Advance powder diffractometer ($K\alpha_{1,2}$ Cu wavelengths). The Rietveld analysis (GSAS software) of the x-ray profiles confirms the trigonal phase with an average purity calculated to be more than 98%. The main phase impurity is the semiconducting cubic $BaSi_2$ presenting the $SrSi_2$-type structure. The three adjustable cell parameters are the two lattice parameters a and c and the z coordinate which represents the $2d$-Wyckoff position of Si atoms ($z = 0.5$ corresponds to completely flat Si planes). Among the different samples, the z coordinate exhibits sizable variations depending on the pressure and on the temperature of synthesis. The two samples presenting the most pronounced structural difference were synthesized at (4.5 GPa, 500 °C) and (4.5 GPa, 1000 °C), and have, respectively, [$a = 4.061(3)$ Å, $c = 5.293(3)$ Å, and $z = 0.565(1)$] and [$a = 4.065(3)$ Å, $c = 5.347(4)$ Å, and $z = 0.546(3)$]. The superconducting transition temperatures T_c of those samples were measured in a SQUID (QD MPMS 5XL). In the left panel of Fig. 2, we can see that the temperature dependence of the zero-field-cooled (ZFC) magnetic susceptibility reveals a T_c onset of 6 K for the phase with $z = 0.565$ and 8.9 K for the one with $z = 0.546$. For the first sample, $[\text{chi}(2\text{ K}) - \text{chi}(10\text{ K})]/H_a = -1.08$ emu/mol per Oe (where H_a is the applied magnetic field = 20 Oe) corresponding to a Meissner superconducting volume fraction of about 27%, typical for bulk superconductivity in sintered samples. For the second sample, with T_c close to 9 K, the dependence of the magnetization on the field evidences a type-II superconductor. As shown in the right panel of Fig. 2, the lower critical field H_{c1} occurs at an applied magnetic field of approximately 50 Oe, corresponding to 75 Oe after correcting for a demagnetization factor of 1/3. We estimate an approximate value of $H_{c2} \sim 7$ kOe. Using the Ginzburg-Landau equations, we obtain for penetration depth $\lambda \sim 3300$ Å and the coherence length $\xi = 104$ Å.

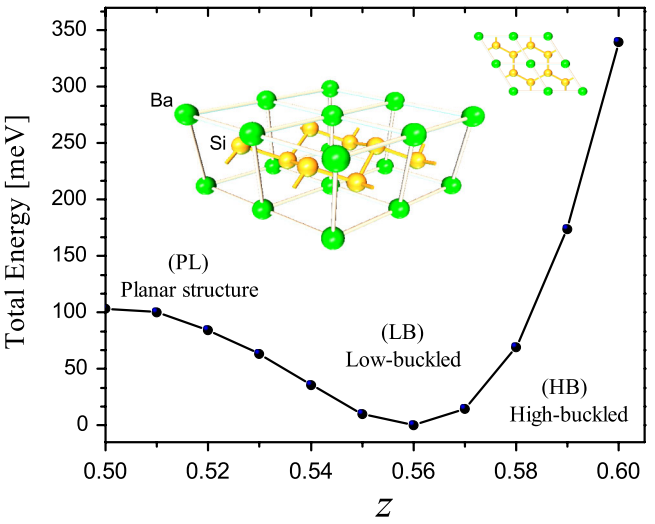

FIG. 1 (color online). Variation of the total energy of trigonal $BaSi_2$ per unit cell as a function of the buckling parameter z, calculated at 0 K. The low-buckled regime $0.545 \lesssim z \lesssim 0.575$ corresponds to the values of z that can be explored experimentally. Inset: (left) Layered structure of $BaSi_2$ ($EuGe_2$-type, P-$3m1$ space group). (right) Projection of the crystal structure onto the (a),(b) plane. The large green (or gray) spheres represent Ba and the small yellow (or light gray) spheres represent Si atoms.

Our DFT calculations were performed with the ABINIT code [19]. The exchange-correlation functional was modeled by a Perdew, Burke, and Erzernhof (PBE) generalized gradient approximation [20], while the electron-ion interaction was described by norm-conserving Troullier-Martins pseudopotentials [21] generated with the same functional. To obtain the phonon dispersion we employed density-functional perturbation theory. Proper convergence was ensured using a cutoff energy of 30 Ha and a 20^3 k mesh with the Monkhorst-Pack sampling of the Brillouin zone. A grid of 4^3 q phonon wave vectors and the tetrahedron technique was used for the integration over the Fermi surface. In the trigonal phase the lowest energy structure of $BaSi_2$, calculated at 0 K, has lattice parameters ($a = 4.08$ Å, $c = 5.42$ Å, and $z = 0.56$ Å). These values are consistent with the experimental parameters within the typical error of PBE calculations [22]. However, by inspection of Fig. 1, we realized that the total energy curve is rather flat in an interval of z, analogously to the case of $CaSi_2$ [23]. We identify three intervals of values of z: a planar region for $z \lesssim 0.545$, a high-buckled interval for $z \gtrsim 0.575$, and a low-buckled interval for $0.545 \lesssim z \lesssim 0.575$. In the low-buckled interval, the total energy changes by less than 50 meV (580 K) per unit cell, explaining why it is easy to deform the structure and obtain experimental samples with different z.

Despite the flatness of the total energy curve, small variations of z in the low-buckled region produce remarkable changes in the electronic structure, in the phonon modes, and in the EP coupling. The Fermi surface,

depicted in Fig. 3(a) is composed of two parts, a larger portion centered at the A point and smaller pockets centered at the M points. The bands composing the former have mostly Si $3p_{xy}$ character, and disperse much more strongly in the xy plane than along vertical directions. Increasing the buckling of the Si-Si bond leads to a shift of these bands, which reduces the size of the Fermi surface [panels (b) and (c)] and, consequently, decreases the value of the density of states at the Fermi level [$N(E_F)$—see panel (d)]. When one reaches $z \gtrsim 0.58$, the interacting orbitals become less confined within the Si layers, forming a weak hybridization between the $5d$ states of Ba and the $3p_z$ of Si. Also the pockets, formed by Ba $5d$ and Si $3p_{xy}$ states, show a light decrease of area upon increase of z, but on a smaller scale than the surface centered at A. For larger values of z (up to 0.6) the Fermi surface does not change significantly from Fig. 3(c). For values of z smaller than 0.55 we can see the appearance of a third sheet of the Fermi surface composed purely of Si $3s$ states. This effect can already be seen in Fig. 3(b) as a tiny yellow dot centered at the A point. Note, however, that for $z < 0.545$ the system becomes structurally unstable, making therefore this region of limited practical importance. Looking at the density of states at the Fermi level [Fig. 3(d)] we see that it attains a maximum in the low-buckled region ($z = 0.545$), then it decreases with increasing z. These numbers already suggest that, from the electronic point of view, superconductivity is favored by smaller values of z.

In order to verify this point, we calculated both the phonon modes and the EP coupling constants as a function of z. At the equilibrium structure our calculated phonon frequencies are close to experimental values. For z close to 0.5, i.e., for almost planar Si layers, the modes exhibit imaginary frequencies indicating a structural instability. In the stable region, most phonon frequencies show only a weak dependence on buckling. However, the A_{1g} optical phonons, which are mainly composed of vibrations of the Si atoms along the c axis (buckling modes), considerably soften upon decreasing z, leading eventually to the structural instability. Moreover, the higher energy E_g mode, composed of Si vibrations in the xy planes, is slightly hardened with decreasing z. In spite of these changes, the value of $\Omega_{\log}$, the weighted average of the phonon frequencies, remains basically unchanged in the range 0.55–0.58, and hence cannot be responsible for the variations of T_c. At $z = 0.56$ we obtain the maximal value $\Omega_{\log} = 182$ K, at $z = 0.55$, $\Omega_{\log} = 170$ K, at $z = 0.545$, $\Omega_{\log}$ drops to 156 K, and at $z = 0.57$ and $z = 0.58$, $\Omega_{\log} = 179$ and 171 K, respectively.

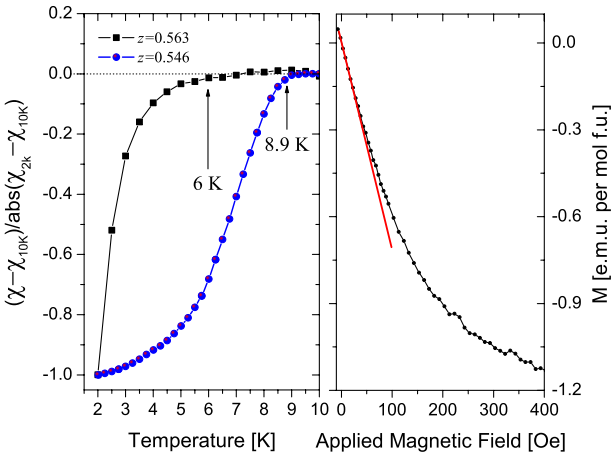

FIG. 2 (color online). Left panel: Temperature dependence of the ZFC dc-magnetic susceptibility measured at 20 Oe of two trigonal samples of $BaSi_2$ marked by their z coordinate. For convenience, we plot the ratio $[\chi(T) - \chi(10\text{ K})]/|[\chi(2\text{ K}) - \chi(10\text{ K})]|$. The arrows indicate the values of T_c obtained at the first point that satisfies the condition $\chi(T) - \chi(10\text{ K}) < -10^{-5}$ emu/mol. Right panel: initial magnetization curve as a function of the applied magnetic field measured at 2 K in the trigonal phase with $z = 0.546(3)$ Å. The upper critical field H_{c2} has been estimated to be 7 kOe, by measuring the magnetic field at which the M-H reverse legs merge at high magnetic field using the criterion $|\Delta M| < 10^{-5}$ emu/mol.

To evaluate the superconducting transition temperature T_c, in the framework of the strong coupling theory of superconductivity [24,25], we need to calculate λ, which measures the average EP interaction. As the calculation of λ involves averaging over the Fermi surface, special care has to be taken to ensure the convergence of results. In fact, an insufficient sampling leads to a dramatic underestimation of T_c [12]. The screened coulomb interaction μ^* was set to 0.1, which is a standard choice for this kind of material. The Eliashberg spectral function $\alpha^2F(\omega)$ is shown in the bottom panel of Fig. 4. There are two main peaks contributing to λ: the first, due to acoustic modes, is fairly insensitive to changes of z; the second, due to the EP coupling of the A_{1g} optical mode, moves to lower frequencies, increasing its area, and consequently its contribution to λ, with decreasing z. In the inset of the bottom panel of

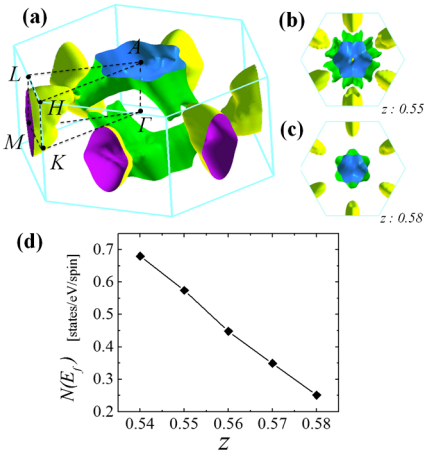

FIG. 3 (color online). (a) Fermi surface of trigonal $BaSi_2$ [27]. (b) and (c) two-dimensional cuts of the Fermi surface perpendicular to the [001] direction for $z = 0.55$ and 0.58. The increase of the Fermi surface when the structure flattens out (smaller z) is evident. (d) Electronic density of states as a function of z.

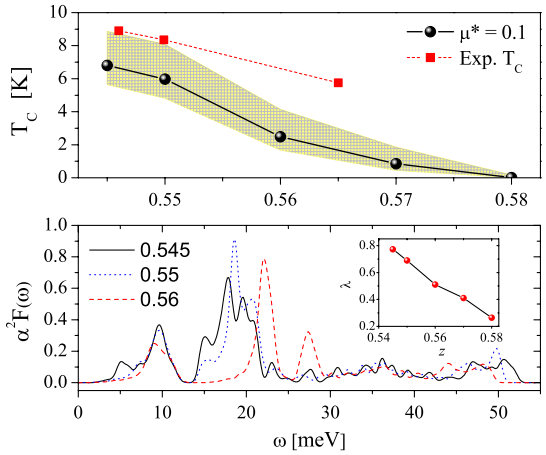

FIG. 4 (color online). Bottom: Eliashberg spectral function $\alpha^2F(\omega)$ (inset: EP coupling constant λ) as a function of z. Top: T_c in K calculated with the McMillan formula. The shaded area shows the T_c values when μ^* varies from 0.06 to 0.125. The squares are the experimental values of T_c.

Fig. 4 one can see how this leads to a pronounced increase of λ with z, and therefore to a maximum theoretical T_c of around 6 K using the McMillian formulation [26] (top panel of Fig. 4). Note that the experimental trend for the dependence of T_c of $BaSi_2$ on the buckling is well reproduced by our calculations, which explain also previous experimental findings for the similar compound $CaSi_2$. The slight underestimation of calculated T_c is due to the neglect of multiband effects that are known to enhance superconductivity in similar systems, such as MgB_2 [4,6].

In conclusion, we presented an experimental and theoretical study of the layered binary silicide $BaSi_2$. We show that the buckling of the Si sheets can be modified experimentally by using different high-pressure and temperature conditions of synthesis. The reason for such a behavior can be found in our DFT calculations, which evidence a broad low-buckling interval where the total energy changes by less than 50 meV (580 K) per unit cell as a function of z. The electronic band structure calculations demonstrate that the density of states at the Fermi level significantly increases by flattening the Si planes. However, such flattening is limited by a structural instability concomitant with the softening of the Si optical buckling phonon mode (A_{1g}). The coupling of this mode with electrons is also dramatically enhanced by flattening the Si planes, leading to the increase (from 6 K up to 8.9 K) of the superconducting transition temperature. Such competition between superconductivity and structural distortion can be found in a wide variety of conventional superconductors, such as the Chevrel phases, the transition metal carbides, the cubic $Ba_{1-x}K_xBiO_3$, etc. This scenario is in full agreement with our experimental and theoretical findings, and it is compatible with previous measurements on the disilicide $CaSi_2$ [15,16]. Moreover, the mechanism of tuning T_c by controlling the buckling of the layers is likely to be present in many other layered superconductors, and therefore can provide a new path for optimizing T_c.

S. B. acknowledges funding from the EC through the e-I3 ETSF Project No. 211956 and MALM from the French ANR (ANR-08-CEXC8-008-01). Calculations were performed at GENCI (Project No. x2011096017). J. A. F. L. acknowledges the program CONACyT-Mexico. We thank D. Machon, R. Viennois, D. Ravot, P. Toulemonde and Y. Sidis for discussions and S. Le Floch for sample preparation. We acknowledge V. Dupuis, M. Hillenkamp, and D. Luneau at the Centre de Magnétomètrie of Lyon for the use of the Squid and R. Vera and E. Jeanneau at the Centre de Diffractomètrie Henri Longchambon for the x-ray measurements at the University of Lyon 1.

[1] O. Chmaissem *et al.*, Nature (London) **397**, 45 (1999).
[2] J. Nagamatsu *et al.*, Nature (London) **410**, 63 (2001).
[3] K.-P. Bohnen, R. Heid, and B. Renker, Phys. Rev. Lett. **86**, 5771 (2001).
[4] A. Y. Liu, I. I. Mazin, and Jens Kortus, Phys. Rev. Lett. **87**, 087005 (2001).
[5] W. Zhou, H. Wu, and T. Yildirim, Phys. Rev. B **76**, 184113 (2007).
[6] M. Calandra and F. Mauri, Phys. Rev. Lett. **95**, 237002 (2005).
[7] S. Kuroiwa *et al.*, Phys. Rev. B **77**, 140503(R) (2008).
[8] G. Q. Huang *et al.*, Phys. Rev. B **71**, 172506 (2005).
[9] J. Evers, J. Solid State Chem. **32**, 77 (1980).
[10] M. Imai and T. Hirano, J. Alloys Compd. **224**, 111 (1995).
[11] M. Imai, K. Hirata, and T. Hirano, Physica C **245C**, 12 (1995).
[12] B. Rousseau and A. Bergara, J. Phys. Conf. Ser. **215**, 012109 (2010).
[13] H. J. Choi *et al.*, Nature (London) **418**, 758 (2002); A. Floris *et al.*, Phys. Rev. Lett. **94**, 37004 (2005).
[14] A. Nakanishi *et al.*, J. Phys. Conf. Ser. **121**, 052010 (2008).
[15] S. Sanfilippo *et al.*, Phys. Rev. B **61**, R3800 (2000).
[16] P. Bordet *et al.*, Phys. Rev. B **62**, 11392 (2000).
[17] M. Imai, T. Hirano, T. Kikegawa, and O. Shimomura, Phys. Rev. B **58**, 11 922 (1998).
[18] M. Imai, T. Hirano, T. Kikegawa, and O. Shimomura, Phys. Rev. B **55**, 132 (1997).
[19] X. Gonze *et al.*, Z. Kristallogr. **220**, 558 (2005).
[20] J. P. Perdew, K. Burke, and M. Ernzerhof, Phys. Rev. Lett. **77**, 3865 (1996).
[21] M. Fuchs *et al.*, Comput. Phys. Commun. **119**, 67 (1999).
[22] Calculations of the total energy curves using the experimental lattice parameters at 500 °C and at 1000 °C confirm that the crystal structure observed at 1000 °C is the most stable.
[23] G. Satta *et al.*, Phys. Rev. B **64**, 104507 (2001).
[24] G. M. Eliashberg, Zh. Eksp. Teor. Fiz. **38**, 966 (1960).
[25] S. Y. Savrasov and D. Y. Savrasov, Phys. Rev. B **54**, 16487 (1996).
[26] W. L. McMillan, Phys. Rev. **167**, 331 (1968).
[27] A. Kokalj, Comput. Mater. Sci. **28**, 155 (2003).